

Mode Profile Shaping with 2D Periodic Array of Metallic Patches on Electrodes in SAW Resonators

Jiman Yoon^{*†1}, Markus Mayer^{†2}, Thomas Ebner^{†3}, Karl Wagner^{†4}, Achim Wixforth^{*5}

^{*} Experimental Physics I, University of Augsburg
Universitätsstr. 1 D-86159 Augsburg, Germany

Email: ¹Jiman.Yoon.external@epcos.com, ¹Ji.man.Yoon@student.uni-augsburg.de

⁵Achim.Wixforth@physik.uni-augsburg.de

[†] Advanced Development Discretes, TDK Corporation,

P.O. Box 80 17 09, 81617 Munich, Germany

Email: ²Markus.Mayer@epcos.com, ³Thomas.Ebner@epcos.com, and ⁴Karl.Wagner@epcos.com

Abstract—Periodic arrays of metallic patches on the electrodes of a Rayleigh-type SAW resonator are investigated to suppress undesired modes above resonance frequency. Both, the metallization ratio (η_t) and the period (p_T) of the patches in transversal direction, were varied. Simulations were performed employing the well established 2D P-matrix model. A well-designed periodic array is capable to suppress all transversal modes within a certain frequency band. The individual transversal modes are well characterized by evaluating the overlap integral of the transversal excitation and mode profile as well as the field strength. From these evaluations it is also possible to understand the mechanism of mode suppression. It has been demonstrated that the modification of the higher symmetric modes caused by patches is responsible for strong spurious peaks in the resonator's frequency response. These results provide insight how the $\Delta v/v$ waveguide, formed by the areas with and without patches, can be engineered to suppress bound and leaky continuum modes.

Keywords— Periodic Array, Spurious Mode, Waveguide, Excitation Strength

I. INTRODUCTION

SAW resonator filters are widely used in the field of telecommunications [1], [2]. Due to the finite aperture of the acoustic track of a resonator, various diffraction effects may occur. Acoustic tracks forming good waveguides show transversal modes propagating under certain angles with respect to the main propagation direction giving rise to undesired peaks in the pass- and the stopband [3], [4]. This inherent attribute deteriorates the characteristics of the frequency response in SAW filters. Various methods have been reported to suppress transversal modes. Aperture weighting can be used to smoothen the transversal mode peaks but this requires additional space and the transversal modes are still excited and the corresponding loss is still existing. A Piston Mode Design fully suppresses all but the fundamental mode [5]. Recently, so-called Phononic Crystals have been proposed for mode suppression in SAW devices [6]. A perfect 2D phononic crystal has a stopband in all directions of the filter surface. Whereas phononic crystals on a macroscopic scale were successfully fabricated, they are not easy to be realized on the micrometer scale [7]. In this work, we investigated 2D periodic arrays of metallic patches on the electrodes in a Rayleigh-type SAW

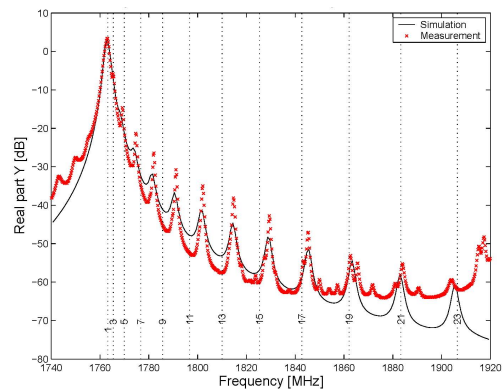


Fig. 1. Y_{12} of a reference one port resonator, Simulation (black) and measurement (red) are in excellent agreement if model parameters for simulation are accurate.

resonator. Both, the metallization ratio and the period of the patches in transversal direction were varied and the resulting effect on the mode spectrum was investigated. Simulations were performed employing the well established 2D P-matrix model. The 2D P-matrix model describes waveguiding and reflection in SAW filters by discretizing acoustic tracks into longitudinal and transversal sections, where free waveguide propagation is assumed within a longitudinal section and reflection is assumed to be concentrated at section boundaries [8], [9], [10]. In Section II, the method of analysis is introduced as well as the principle of mode suppression. In section III, the modal decomposition of the excitation strength is dealt with to analyse spurious mode suppression.

II. APPROACH

It is well known that the excitation of the transversal spurious modes originates from the different shapes of the transversal electroacoustic transduction profile and the fundamental symmetric mode [5], [11]. The former is usually rectangular-like, while the latter differs from case to case. As mentioned in the previous section, popular methods to control spurious modes are Aperture Weighting, where the average excitation profile resembles the fundamental mode and

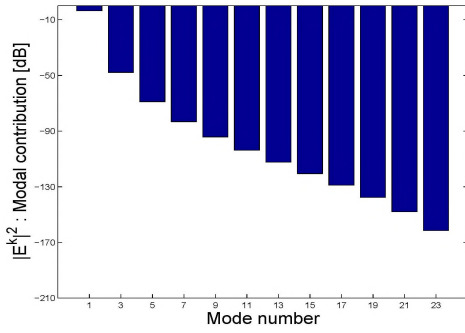


Fig. 2. Excitation strengths of transversal modes. Only symmetric modes are shown on the bar plot since the anti symmetric mode cancel out.

a Piston Mode device, where a rectangular fundamental mode, ψ_1 , is enforced [11]. In principle, the 2D P-matrix method allows to represent the conductance as the sum of modal contributions [9]. However, this method is a bit complicated to be interpreted directly. A simple scheme to guess the position of peaks originating from higher transversal modes is the assumption of sinusoidal modes in a velocity profile with infinitely high walls, [4], where the parabolic approximation is assumed and mode coupling by reflection is not considered, i.e.,

$$k_x^2 + k_y^2(1 + \gamma) = k_0^2 \quad (1)$$

where $k_x = \frac{\pi}{p_L}$, the wave number of longitudinal periodicity (p_L) of active fingers, $k_y = \frac{\pi}{A} \cdot m$, and A is the aperture of the waveguide. γ is the anisotropy coefficient and is assumed to be constant. $k_0 = \frac{2\pi f_m}{v_0}$ is the wave number in x -direction, where v_0 is the velocity in x -direction and f_m is the frequency of mode m . By solving the above equation for f_m we obtain;

$$f_m = f_0 \sqrt{1 + \left(\frac{p_L m}{A}\right)^2 (1 + \gamma)}, \quad (2)$$

where $f_0 = \frac{v_0}{2p_L}$ is the resonance frequency for the one dimensional case. Since the coupling is neglected in this simple approximation, deviations from the peak positions become larger the higher the mode numbers are (Fig 1). For the low lying transversal modes, contrarily, the positions of the peaks are predicted quite precisely.

To investigate the symmetric modal contribution of the observed peaks, we have to look at the excitation strength of each mode. The excitation strength of the k^{th} mode is the scalar product of excitation profile and mode profile over the transversal direction [11], i.e.,

$$E^k = \langle e(y) | \psi^k(y) \rangle = \int_{-\frac{A}{2}}^{\frac{A}{2}} e(y) \cdot \psi^k(y) dy, \quad (3)$$

where $e(y)$ and $\psi^k(y)$ are the transversal excitation and mode profile of the k^{th} mode, respectively. Both functions, $e(y)$ and $\psi^k(y)$, are normalized. Since antisymmetric modes

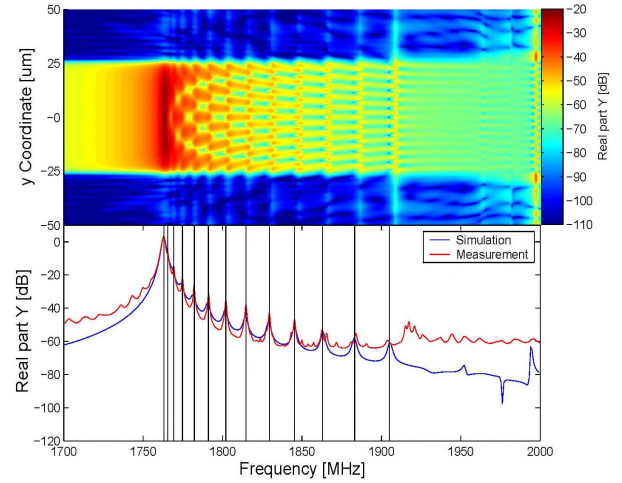


Fig. 3. Field strength over the complete frequency range (top) and conductance frequency response (bottom). Supplementary vertical lines indicate spurious peaks.

are cancelled out, only the symmetric transversal modes are visible in the spectrum. Hence, only the symmetric modes are indicated in Fig 1.

III. ANALYSIS

We study the effect of 2D periodic patches on electrodes for one port resonators with 5 different periods for the patch and 6 different patch metallization ratios. A one-port resonator without patches serves as reference structure. $128^\circ Y - X LiNbO_3$ is chosen as a substrate material, where the surface of the substrate is coated with SiO_2 . For the electrodes and patches, the same kind of metallization is used. Here, we mainly discuss the analysis of two resonators; one is the reference and the other one is the case with the optimum mode suppression. The comparison is good enough to grasp the principle of mode suppression by the periodic array. First we consider the reference structure.

A. One Port Resonator: Reference Structure

Over the entire active aperture, the transversal metallization ratio is homogeneous. Therefore the transversal excitation profile is given by;

$$e = \begin{cases} e_0 & y \in \left[-\frac{A}{2}, \frac{A}{2}\right] \\ 0 & else \end{cases}. \quad (4)$$

However, in general, the excitation profile is frequency dependent and can be obtained from 2D P-matrix computation [11]. In the calculation of modal contributions to admittance, Eq. (3) and (4) are used and the frequency dependency of the excitation and mode profile is considered (Fig. 2). In Fig. 1, the fundamental mode dominates the conductance characteristics. The 1^{st} symmetric mode is very close to the fundamental mode and nearly fully covered by it. Although the subsequent modes have lower and lower excitation strength, they are better visible in the conductance since they are located at frequencies with

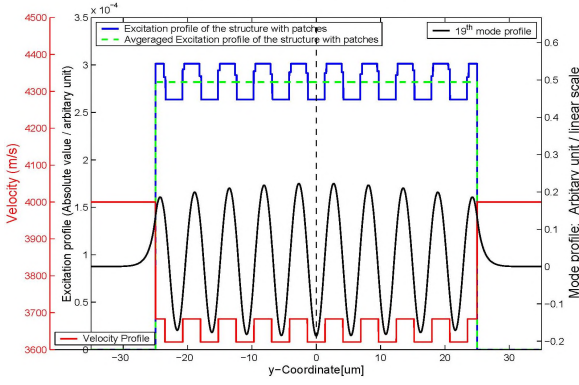


Fig. 4. Excitation profile of the structure with patches (blue) and the averaged excitation profile (green) of it, velocity profile (red), and the 19th mode profile (black). Each of them is scaled for ease of comparison.

lower conductance level of the fundamental mode.

On the other hand, the simulation based on the 2D P-matrix is capable to compute the field strength. In this model, a unit cell is defined with 2 strips, which then is infinitely cascaded taking into account reflection and diffraction [8], [9], [10]. The field strength over the complete frequency range is visualized in Fig. 3. Interestingly, in Fig. 3 top, the number of nodes in the field strength increases as the frequency increases. Spurious peaks are located at frequencies, where the number of nodes starts to change. Therefore Fig. 3 provides us with the insight of the responsible transversal mode for the peaks (Fig. 3 bottom).

B. Resonator with 2D Periodic Array

We now turn to the investigation of a resonator with 11 patches in the active track region. The excitation profile of the resonator with the 2D periodic patches on the electrodes is no longer homogeneous over the entire transversal aperture unlike the reference resonator (Fig. 4 blue line). Therefore the excitation profile is given by

$$e = \begin{cases} e_0 & y \in \mathbf{T} \\ e_1 & y \in \mathbf{P} \\ 0 & \text{else} \end{cases}, \quad (5)$$

where \mathbf{T} and \mathbf{P} are the regular region and the region with patches, respectively. In addition, the velocity profile over the transversal aperture is also not homogeneous owing to the patches. As a result, the mode profile for the k^{th} mode is also changed. The contribution of the k^{th} transversal mode to the conductance is computed now by Eq. (3) using Eq. (5) and the new mode profile, $\psi_{\mathbf{D}}^k(\mathbf{y})$ (Fig. 5 blue bars). In Fig. 5, the modal contribution by the 2nd and 3rd symmetric mode are similar to the ones on Fig. 2, respectively. In the frequency characteristics of the conductance these modes are fully covered by the fundamental mode and hardly visible in both cases (Fig. 3 and 6).

The decrease of the excitation strength from the 5th symmetric mode to the 11th is larger than the one in Fig. 2, which means the spurious peaks are well suppressed in this region (Fig. 6 bottom). In Fig. 5, the modal contribution from

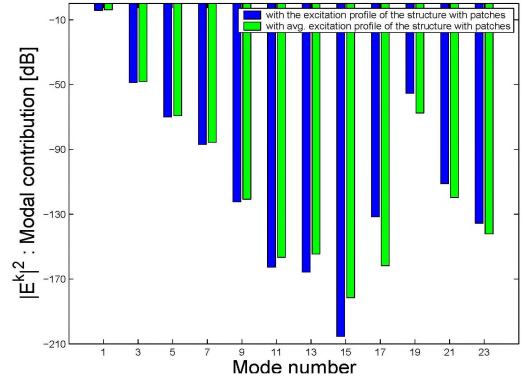


Fig. 5. Transversal modal contribution on spurious peaks. Computation results with the excitation profile of the structure with patches (blue bars) and with the averaged excitation profile (green bars) are plotted respectively.

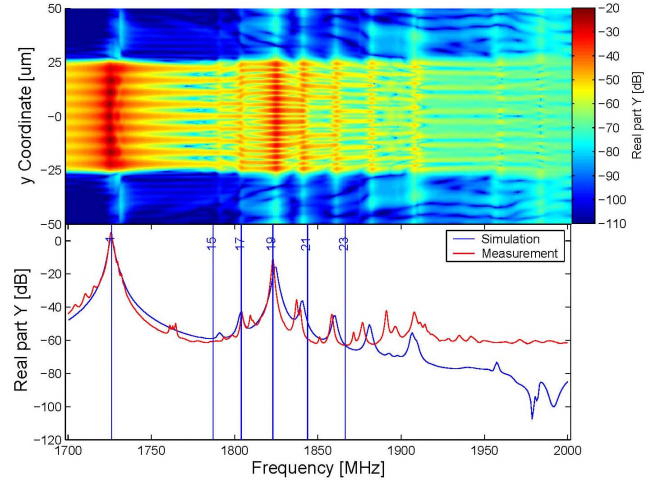


Fig. 6. Field strength over the complete frequency range (top) and frequency response on conductance (bottom).

the 9th symmetric mode (17th mode) to the 12th symmetric mode (23rd mode) is strongly increased so that the spurious peaks caused by these modes are observable in the frequency response of conductance (Fig. 6 bottom). Especially the peak on the 19th mode position is very strong in agreement with Fig. 5, where the modal contribution is large.

In Fig. 6 top unlike to Fig. 3 top, up to the resonance frequency of the 15th mode, no change in the field pattern is visible; rather the profile resembles the fundamental mode of the structure with patches. This is consistent with a reasonable mode suppression. The spurious peaks appear where the transitions to the next higher modes take place.

Nevertheless, it is still unclear whether the strong peaks are caused by the excitation profile or the modified mode profile. To identify the primary reason, the modal contribution is computed using the averaged excitation profile (Fig. 4 dotted green line), Eq. (6) instead of using Eq. (5),

$$e = \begin{cases} e_{avg} = \frac{e_0 + e_1}{2} & y \in \mathbf{T} \text{ and } \mathbf{P} \\ 0 & \text{else} \end{cases}, \quad (6)$$

where \mathbf{T} and \mathbf{P} are the regular region and the region with

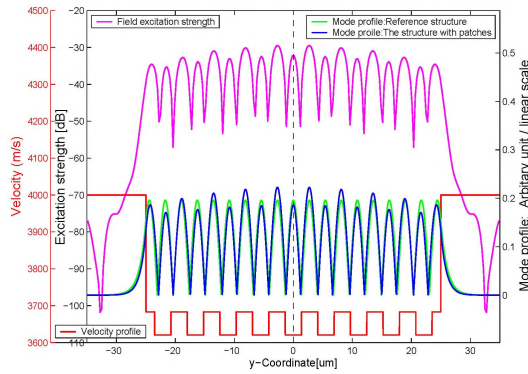


Fig. 7. Field strength for the frequency corresponding to the 19th mode (magenta), velocity profile (red) and the 19th mode profiles for reference (green) and the structure with patch (blue). The mode profiles are plotted in absolute value. Each of them is scaled for ease of comparison.

patches, respectively. As can be seen in Fig. 5, the modal contribution (green bars) reveals qualitatively the same result to the one with Eq. (5).

In Fig. 7, the field strength at the frequency corresponding to the 19th mode and velocity profile of the structure with patches, and the mode profiles for both the reference structure and the structure with patches are respectively plotted over transversal direction. Each of them is scaled in order to make a comparison possible. As can be seen, the mode profile of the structure with patches is somewhat more concentrated in the center of the track than the mode profile of the reference. The magnitude of the upper lobes and the corresponding lower lobes becomes unequal. Consequently, the resulting value of the overlap integral by Eq.(3) increases considerably. The mode responsible for the excitation is the one which has the same number of maxima and minima as the transversal velocity profile produced by the periodic array of metal patches. This equal periodicity and the velocity profile by patches result in the modification of the 19th mode profile and consequently the strong spurious peak in the frequency response on conductance in Fig. 6 bottom. Note that, at each transition point in Fig. 6 top, radiation towards the transversal direction takes place and is especially large for the 19th mode. It is worth noting that the frequency position of the 19th mode agrees well with the one predicted even if neglecting any mode conversion. This may be due to the fact that the mode and reflection profile are very similar and therefore little mode conversion occurs.

IV. CONCLUSION AND DISCUSSION

We have fabricated one-port resonators with 2D periodic metal patches on the top of the electrodes. Admittances and field distributions were computed using the 2D P-matrix model. The individual transversal modes are well characterized by evaluating the overlap integral of the transversal excitation and mode profile as well as the field strength. From these evaluations it is also possible to understand the mechanism of mode suppression.

In this work, it is demonstrated that a 2D periodic array can be successfully employed to suppress undesired modes

within the frequency band for $k_y = \left[0, \frac{\pi}{p_T} \right]$. The frequency band can be engineered by the pitch of the transversal patch. It is also demonstrated that the modification of the higher symmetric modes caused by patches is responsible for strong spurious peaks in the resonator's frequency response. These results provide insight how the $\Delta v/v$ waveguide, formed by the areas with and without patches, can be engineered to suppress bound and leaky continuum modes. Alternatively it is possible to consider other simple periodic structures resulting in a similar waveguiding effect like patches directly on top of the electrodes. Such alternative periodic modulations of the transducer electrodes are presently under investigation and will be discussed elsewhere.

ACKNOWLEDGMENT

The authors would like to deliver special thanks to Mr. H. Zottl, Mr. S. Berek, Mr. H. Oetzuerk for the fabrication of samples and the measurement.

REFERENCES

- [1] C. Ruppel, R. Dill, A. Fischerauer, G. Fischerauer, A. Gawlik, J. Machui, F. Muller, L. Reindl, W. Ruile, G. Scholl, I. Schropp, and K. Wagner, "Saw devices for consumer communication applications," *Ultrasonics, Ferroelectrics and Frequency Control, IEEE Transactions on*, vol. 40, no. 5, pp. 438–452, sept. 1993.
- [2] C. Campbell, "RF Design", *One-port leaky-SAW resonators: building blocks for low-loss RF front-end systems*, 1999.
- [3] N. Pocksteiner, M. Jungwirth, G. Kovacs, and R. Weigel, "Analysis of general planar waveguides with n segments," in *Ultrasonics Symposium, 2000 IEEE*, vol. 1, oct 2000, pp. 137–141 vol.1.
- [4] S. Rooth and A. Ronnekleiv, "Saw propagation and reflections in transducers behaving as waveguides in the sense of supporting bound and leaky modes," in *Ultrasonics Symposium, 1996. Proceedings., 1996 IEEE*, vol. 1, nov 1996, pp. 201–206 vol.1.
- [5] M. Mayer, A. Bergmann, G. Kovacs, and K. Wagner, "Low loss recursive filters for basestation applications without spurious modes," in *Ultrasonics Symposium, 2005 IEEE*, vol. 2. IEEE, 2005, pp. 1061–1064.
- [6] M. Solal, J. Gratier, and T. Kook, "A saw resonator with two-dimensional reflectors," in *Frequency Control Symposium, 2009 Joint with the 22nd European Frequency and Time forum. IEEE International*. IEEE, 2009, pp. 226–231.
- [7] V. Laude, M. Wilm, S. Benchabane, and A. Khelif, "Full band gap for surface acoustic waves in a piezoelectric phononic crystal," *Phys. Rev. E*, vol. 71, p. 036607, Mar 2005. [Online]. Available: <http://link.aps.org/doi/10.1103/PhysRevE.71.036607>
- [8] M. Mayer, G. Kovacs, A. Bergmann, and K. Wagner, "A powerful novel method for the simulation of waveguiding in saw devices," in *Ultrasonics, 2003 IEEE Symposium on*, vol. 1, oct. 2003, pp. 720–723 Vol.1.
- [9] K. Wagner, M. Mayer, A. Bergmann, and G. Riha, "A 2d p-matrix model for the simulation of waveguiding and diffraction in saw components (invited)," in *Ultrasonics Symposium, 2006. IEEE*, oct. 2006, pp. 380–388.
- [10] G. Kovacs, "A generalised p-matrix model for saw filters," in *Ultrasonics, 2003 IEEE Symposium on*, vol. 1, oct. 2003, pp. 707–710 Vol.1.
- [11] M. Mayer, A. Bergmann, K. Wagner, M. Schemies, T. Telgmann, and A. Glas, "Low resistance quartz resonators for automotive applications without spurious modes," in *Ultrasonics Symposium, 2004 IEEE*, vol. 2. IEEE, 2004, pp. 1326–1329.